

P.S. Virk and V.J. Vlastnik
 Department of Chemical Engineering
 M. I. T., Cambridge, MA 02139

KEYWORDS: Thermolysis, Reaction Paths, Kinetics, Demethylation, Hydrogen Transfer.

INTRODUCTION

Motivation. This work on thermolysis of 9-methyl-anthracene, abbr 9MA, is a part of our continuing studies of methylated acenes, that mimic the chemical moieties found in complex fossil materials of engineering interest. Also, since 9MA is a primary product of 9,10-dimethyl-anthracene, abbr 910DMA, thermolysis [1, 2], it was hoped that information regarding the former might buttress our understanding [3] of 910DMA thermolyses at high conversions.

Previous Work. The earliest work we could find on 9MA thermolysis was by Pomerantz [4], who reported its half-life to be ~ 25000 s at $T = 400$ C for an initial concentration $[9MA]_0 \sim 0.15$ mol/l, with anthracene, abbr ANT, as the major product, accompanied by lesser amounts of 1- and 2-methyl-anthracenes, abbr 1MA, 2MA, and 9,10-dihydro-anthracene, abbr DHA. Subsequently, in a brief experimental and mechanistic study of 910DMA thermolysis at $310 < T < 390$, conducted in the present authors' laboratory, Pope [5] pointed out that 9MA can give rise to two delocalized radicals,



 HMA9* and HMA10*, of which only the latter can propagate the demethylation pathway to ANT. Most recently, Smith & Savage [6] have pyrolysed 9MA at $350 < T < 400$ using $[9MA]_0 \sim 0.09$ mol/l. Their decomposition kinetics were ~ 20 -fold faster than those reported by Pomerantz [4] and they detected dimethyl-anthracenes, abbr DMAs, among the products, in addition to the ANT, 1MA, 2MA and DHA previously found.

Outline. We first describe the experiments and present results for the concentration histories, product selectivities, and kinetics observed during 9MA thermolysis. Reaction pathways for the decomposition of 9MA are then inferred from the major products observed, and their ratios. Finally, a free-radical mechanism comprising 22 elementary steps is proposed for 9MA thermolysis at low conversions, and shown to accommodate many of the experimental observations.

EXPERIMENTAL

Conditions. Table 1 summarizes conditions for, and results obtained from, the present experiments. The first column of this table refers to 9MA substrate and its second to 910DMA, the latter serving as a basis for later comparisons. The upper portion of Table 1 summarizes conditions for the experiments, listing the model substrates, their structures and the ranges of temperatures, holding times and initial concentrations studied, as well as the temperatures at which light gases were analysed. Thermolyses were conducted in batch reactors, volume 0.6 ml, made from 1/4" stainless steel Swagelok parts. The reactors were charged with weighed amounts of biphenyl (internal standard) and substrate (9MA) totalling 0.30 g, sealed and placed in an isothermal, fluidized-sand bath for the appropriate holding times, after which they were quenched in ice-water, and their contents extracted into methylene chloride. Reactor contents were in the liquid phase during all experiments.

Assays. Gaseous and liquid thermolysis products were identified and analyzed by GC, augmented by GC/MS. All gas peaks were identified by injections of standards. Most liquid products were identified by injections of standards with some minor liquid products identified by determining their masses by GC/MS and relating their retention times to those of known molecules. Heavy thermolysis products, mostly dehydrogenated dimers of the substrates, were identified by GC/MS. For example, in 9MA thermolyses, the MS of a prominent late GC peak showed a molecular ion at mass 382 and a fragment at mass 191, suggestive of a bibenzylidene, dehydrogenated dimer of 9MA called 9MAD. Product assay trains developed for 9MA substrate using the preceding GC and GC/MS techniques typically identified ~ 15 reaction products. Identified products accounted for $> 70\%$ of the reacted mass at substrate fractional conversions $0.2 < X < 0.8$. Experimental details are available [7].

RESULTS and DISCUSSION

Histories. Fig. 1 chronicles the concentration histories of substrate and products during thermolysis of 9MA at $T = 370$ C and $[C]_0 = 0.82$ mol/l, using arithmetic coordinates of absolute mols J of either substrate or product present in the reactor versus reaction holding time t in seconds. Part (a), upper panel, shows that the substrate 9MA decayed monotonically, with half-life $t^* \sim 23000$ s. The products formed, in order of their abundance, were ANT, various dimethyl-anthracenes, abbr ALL DMAs, methane CH₄, 1MA, 2MA, and trimethyl-anthracenes, abbr TMA. Part (b), lower panel, details histories of the individually identified dimethyl-anthracene isomers and several 9,10 dihydro- species. The DMAs include 9,10-DMA (major), and 1,10-, 1,9-, and 2,9- + 3,9-DMA, while the hydrogenated species are DHMA (major), DHDMA, and DHA. The formation of DMAs and DHMA products concurrent with ANT shows that during 9MA thermolysis, methylation and hydrogenation always occur in parallel with demethylation. It is also interesting that the isomers 1MA and 2MA both arose subsequent to ANT, which suggests that they formed from methylation of ANT rather than from the isomerization of 9MA.

Selectivities. Fig. 2 depicts the preceding product history data as selectivity diagrams, with ordinate of product selectivity $S = \text{mols J produced/mol of substrate 910DMA decomposed}$, and abscissa of substrate fractional conversion X . Parts (a), upper panel, and (b), lower panel, show that the products formed at low conversions, $X < 0.30$, were ANT, DMAs, DHMA, and CH_4 with selectivities respectively $S = 0.30, 0.20, \sim 0.10$ and 0.05 . With increasing conversions, to $X \sim 0.60$, the selectivity to ANT increased somewhat, to $S \sim 0.35$; the DMAs showed a shallow maximum, $S \sim 0.20$ at $X \sim 0.4$ and then declined slightly; DHMA declined sharply, to $S \sim 0.03$ at $X \sim 0.6$, and CH_4 increased monotonically, to $S \sim 0.15$ at $X \sim 0.6$. The sum of the selectivities of all identified liquid products (squares) was ~ 0.75 over the major range of conversions, $0.2 < X < 0.6$, from which the selectivity of unidentified, mostly heavy, product formation is inferred to be ~ -0.25 .

Kinetics. 9MA decomposition kinetics are illustrated in Fig. 3. Part (a), upper panel, is a log-log plot of decay half-life t^* versus initial concentration $[9\text{MA}]_0$ at fixed temperature. The data, spanning 1.5 decades of $[9\text{MA}]_0$, describe a line of slope $-1/2$, which implies that the decomposition was of 3/2 order wrt substrate. Part (b), bottom panel, is an Arrhenius type of semi-log plot, showing decay half-life t^* versus the reciprocal of a scaled absolute temperature $\Theta = 0.004573^*(T\text{ C} + 273.2)$. Here the data span almost two decades of t^* and lie on a line of slope ~ -46 , which latter is directly the activation energy of decomposition E^* , kcal/mol. The observed kinetics are summarized in Table 1, which shows decay half-lives at $T = 370\text{ C}$, orders wrt substrate, and Arrhenius parameters ($\log A, E^*$). Both the decompositions of 9MA and of 910DMA are of 3/2 order wrt the substrate and exhibit activation energies ~ 45 kcal/mol; their relative decomposition rates are roughly in the ratio 1 : 2.

Product Ratios. The importance of each of the observed hydrogenation, methylation, and methane formation pathways relative to the dominant demethylation pathway can be assessed from the respective primary product ratios R , namely $R[\text{DHMA}/\text{ANT}]$, $R[\text{DMAs}/\text{ANT}]$ and $R[\text{CH}_4/\text{ANT}]$. Of these, the ratio of hydrogenation to demethylation $R[\text{DHMA}/\text{ANT}] \rightarrow 0.7$ at the lowest conversions, $X \rightarrow 0$, and then decreased rapidly to 0.05 ± 0.025 for $0.20 < X < 0.75$; this variation of $R[\text{DHMA}/\text{ANT}]$ versus X was essentially independent of initial concentration and temperature. Fig. 4(a), left panel, shows that the ratio of methylation to demethylation $R[\text{DMAs}/\text{ANT}] \sim 0.8 \pm 0.1$ for $X < 0.3$ at all temperatures while Fig. 4(b), right panel, shows that the ratio of methane formation to demethylation $R[\text{CH}_4/\text{ANT}] = 0.20 \pm 0.03$ for $X < 0.3$ at $T = 370\text{ C}$. The sum $R[\text{DMAs}/\text{ANT}] + R[\text{CH}_4/\text{ANT}] \sim 1.0$ was close to unity, accounting for the methyl radicals implicitly associated with the demethylation pathway. Thus, at low substrate conversions, $\sim 1/5$ of all methyl radicals formed were quenched by hydrogen abstraction, forming methane gas, while $\sim 4/5$ were trapped by addition to the 9MA substrate, eventually appearing as DMAs. These results for 9MA substrate are in striking contrast to those for 910DMA [3], wherein $\sim 3/4$ of methyl radicals were quenched by hydrogen abstraction while $\sim 1/4$ were trapped by addition to the substrate. Since 9MA and 910DMA respectively possess 3 and 6 benzylic H-atoms per molecule, the observed [H-abstraction/addition] ratios of $1/4$ versus $3/1$ show the methyl addition affinity of 9MA to be 6-fold greater than that of 910DMA. The greater methyl affinity of 9MA relative to 910DMA likely derives from the potency of its unsubstituted 10-position as an addition site.

Pathways. The foregoing observations lead to the 9MA decomposition pathways depicted in Fig. 5. Three primary pathways operate in parallel: (P1) Hydrogenation, to DHMA, (P2) Demethylation, to ANT, and (P3) Methylation, to 910DMA. Too, the demethylated acene product is associated with formation of methane gas CH_4 , and the scheme also includes formation of a heavy bibenzylidic dimer of 9MA called 9MAD. Further, the primary demethylation and methylation products shown in the above scheme can be secondarily operated upon by a pathway triad analogous to the one from which they arose, leading, recursively, to the formation of a variety of methylated and hydrogenated acenes. This is evident in the appearance, at high conversions, of TMAs, a host of DMAs, 1MA and 2MA, as well as DHA and DHDMA (for clarity, these secondary products were omitted from Fig. 5). Pathway results are summarized in the bottom of Table 1, which shows major product selectivities and ratios at $T = 370\text{ C}$ and conversions $X = 0.05$ and 0.4 . Results for 9MA were akin to those obtained for 910DMA, but showed a two-fold greater selectivity to the methylated product, and also roughly two-fold greater ratios of hydrogenated/demethylated and of methylated/demethylated products at low conversions.

Mechanism. A possible mechanism for 9MA thermolysis is presented in Fig. 6, an elementary step "graph" constructed with substrate and all stable molecular products arrayed in the bottom row and unstable radical intermediates arrayed in the top row. Reaction "nodes", in the middle row, connect the individual species in the bottom and top rows with arrows indicating the initial direction of reaction (all reactions are reversible). Initiation reactions are denoted by solid interconnecting lines, propagation reactions by dashed lines and termination reactions by dotted lines. The 9MA substrate is in the middle of the bottom row, with light (propagation) products to its right and heavy (termination) products to its left. Consider first a subset of the full mechanism comprising reactions (R1-R10). This free-radical cycle is initiated by the bimolecular disproportionation of substrate (R1), an intermolecular hydrogen transfer reaction, to form the respectively dehydrogenated and hydrogenated radical species 9MA^* and $\text{HMA}10^*$. Of these, the latter can either abstract hydrogen from 9MA by (R2), to form DHMA product, or undergo a β -scission type of radical decomposition by (R3), forming ANT product and a methyl radical CH_3^* . The CH_3^* can either abstract H from 9MA by (R4), to form methane product, or add to 9MA by (R5), to form the dimethyl radical HDMA^* . The latter can then abstract H from 9MA via (R6) to form the observed 910DMA product. The cycle is terminated by the species 9MA^* and $\text{HMA}10^*$ engaging in both pure- and cross-combinations, (R7-R9), to form various dimeric products. $\text{HMA}10^*$

radical can also terminate by disproportionation, (R10), to form 9MA and DHMA. The foregoing portion of the full 9MA mechanism is evidently analogous to the 910DMA mechanism devised earlier [2, 3]. However, the 9MA substrate permits formation of an additional radical, HMA9*, which can engage in all the steps shown for HMA10* except for C-C bond scission, giving rise to steps (R11-R22) of the full mechanism. Thus substrate disproportionation by (R11) forms 9MA* and HMA9*, of which the latter can abstract hydrogen from 9MA by (R12), to form DHMA product. HMA9* can also form from H-transfer reactions (R16), between HDMA* and 9MA, and (R17), between HMA10* and 9MA, the latter causing radical isomerization. Finally, HMA9* can engage in a variety of termination reactions, including pure- and cross-combinations (R18, R19, R21) that form dimeric products, and disproportionations (R20, R22) that form 9MA and DHMA.

The proposed mechanism accounts for the major products, ANT, DMAs, DHMA, CH4 and heavies, observed during the initial stages of 9MA thermolysis. Each of the observed triad of primary pathways, namely, P1 hydrogenation, P2 demethylation and P3 methylation, also arise naturally as limiting cases of the elementary step graph, with P1 comprising the sets [R1, R2, R7] and [R11, R12, R7], P2 the set [R1, R3, R4, R7] and P3 the set [R1, R3, R5, R6, R7]. The stoichiometry of these sets restricts the maximum selectivity of each major product to 1/3, which is of the magnitude of the highest selectivities actually observed. The mechanism also offers some theoretical insights. It suggests that the relative kinetics of hydrogenation to demethylation, (P1)/(P2), are controlled by the HMA9* and HMA10* radicals. The HMA10* radical propagates both hydrogenation (R2) and demethylation (R3), but HMA9* propagates only hydrogenation (R12). It follows that the pathway ratio (P1)/(P2) = [(R2)+(R12)]/(R3) for 9MA should exceed that for 910DMA, which has only a single radical carrier analogous to HMA10*. This accords with the observations in Table 1, which show (P1)/(P2) for 9MA almost twice that for 910DMA at low X. Further, the methylation to demethylation ratio, (P3)/(P2), is essentially governed by competition between methyl radical reactions (R4) and (R5), in which CH₃* either abstracts H from or adds to the 9MA substrate. In this regard, H-abstraction from 9MA should be less favoured than that from 910DMA by a statistical factor of 2, but 9MA possesses a potent unsubstituted 10-position in addition to all the unsubstituted positions present in 910DMA, so methyl radical addition to 9MA should be greatly favoured over that to 910DMA. Theoretically, therefore, the pathway ratio (P3)/(P2) for 9MA should exceed that for 910DMA. This accords with observations in Table 1 which show (P3)/(P2) for 9MA from 1.5 to 2 times that for 910DMA over the entire range of substrate conversions.

In future work it is hoped that the mechanism presented above will provide a basis for the further quantitative modelling and numerical simulation of 9MA and 910DMA thermolyses.

ACKNOWLEDGEMENT: This work was supported in part by Cabot Corporation, Boston, MA.

REFERENCES

- [1] Virk, P.S.; Vlastnik, V.J.: PREPRINTS, Div. of Fuel Chem., ACS, 37(2), 947 (1992).
- [2] Virk, P.S.; Vlastnik, V.J.: PREPRINTS, Div. of Petrol. Chem., ACS, 28(2), 422 (1993).
- [3] Virk, P.S.; Vlastnik, V.J.: PREPRINTS, Div. of Fuel Chem., ACS, 32(2), 546 (1994).
- [4] Pomerantz, M.; Combs Jr., G.L.; Fink, R.: J. Org. Chem., 45, 143 (1980).
- [5] Pope, J.M.: Ph.D. Thesis, Dept. of Chem. Eng., MIT, Cambridge, MA (1987).
- [6] Smith, C.M.; Savage, P.E.: A.I.Ch.E. J., 39, 1355 (1993).
- [7] Vlastnik, V.J.: Sc.D. Thesis, Dept. of Chem. Eng., MIT, Cambridge, MA (1993).

Table 1. Experimental Grid, Kinetics, and Major Product Selectivities and Ratios for Thermolyses of 9MA and 910DMA.

Substrate Structure	9MA	910DMA	
			
Experimental Grid			
Temperature, T C	315-409	315-409	
Holding Time, t s	450-57600	450-57600	
Initial Concentration, [C] ₀ , mol/l	0.082-2.06	0.082-2.47	
Gas Analyses at T C	370	335, 370	
Kinetics			
Decay Half-Life, t* s at T = 370 C	23000	9900	
Order wrt substrate	1.50	1.53	
Arrhenius Parameters (log A, E*)	(11.4, 46.4)	(10.6, 43.1)	
Product Selectivities at T = 370 C	X		
Demethylated	0.4	0.37	0.42
Methylated	0.4	0.22	0.10
Hydrogenated	0.05	0.03	0.06
Heavies	0.4	0.13	0.15
Product Ratios at T = 370 C	X		
[Hydrogenated/Demethylated]	0.05	0.43	0.21
	0.4	0.05	0.04
[Methylated/Demethylated]	0.05	0.69	0.35
	0.4	0.59	0.24

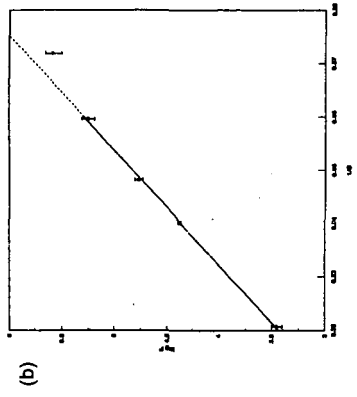
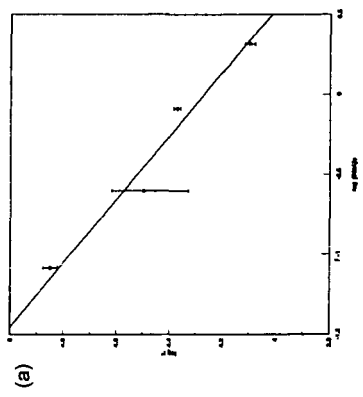


Fig. 3. 9MA thermolysis kinetics.
 (a) Effect of $[9MA]_0$ at fixed $T = 370$ C.
 (b) Arrhenius diagram for fixed $[9MA]_0 = 0.82$ mol/l.

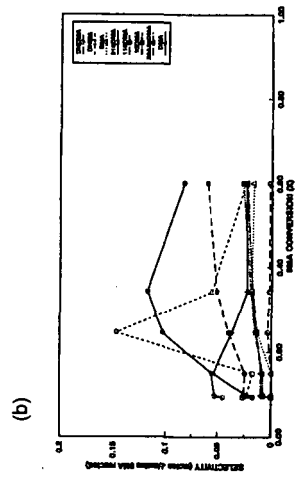
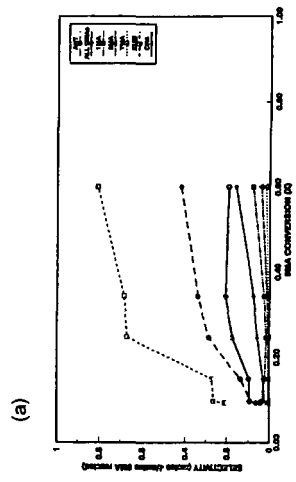


Fig. 2. Product selectivities for 9MA thermolysis at $T = 370$ C, $[9MA]_0 = 0.82$ mol/l.
 (a) ANT, DMAS, 1MA, 2MA, TMA, SUM, CH4.
 (b) All other products.

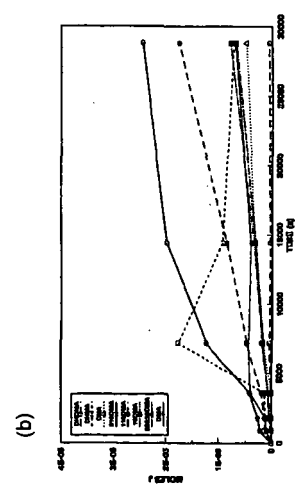
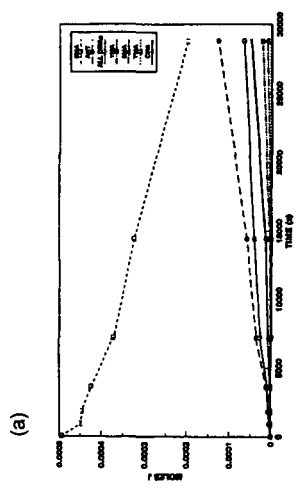


Fig. 1. Substrate and product histories for 9MA thermolysis at $T = 370$ C, $[9MA]_0 = 0.82$ mol/l.
 (a) 9MA, ANT, DMAS, 1MA, 2MA, TMA, CH4.
 (b) All other products.

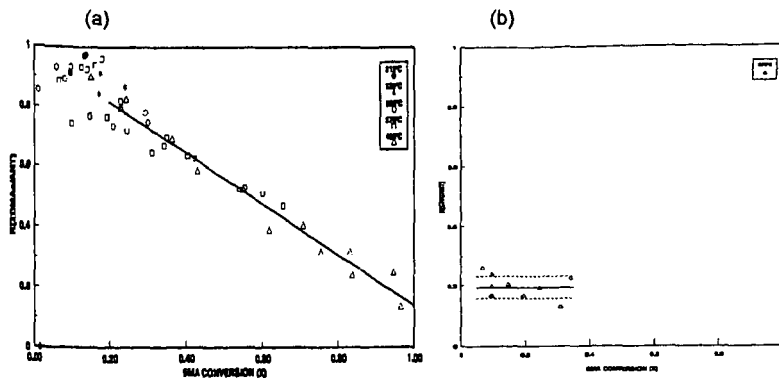


Fig. 4. Major product ratios in 9MA Thermolyses.
 (a) $R[\text{DMA}/\text{ANT}]$ at $T = 315$ to 409 C and $[\text{9MA}]_0 = 0.82$ mol/l.
 (b) $R[\text{CH}_4/\text{ANT}]$ at $T = 370$ C and $[\text{9MA}]_0 = 0.82$ mol/l.

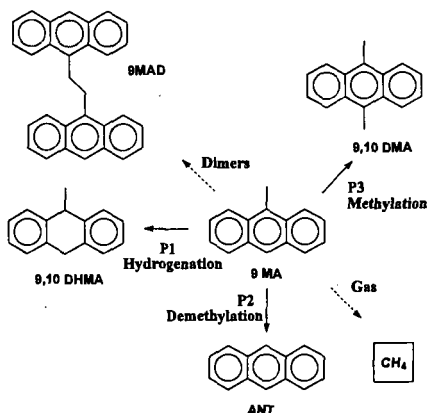


Fig. 5. Major pathways in 9MA thermolysis.

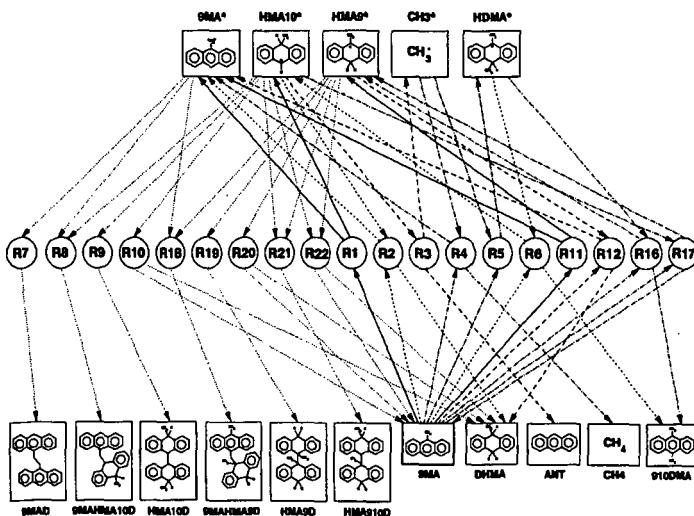


Fig. 6. Elementary step graph of 9MA thermolysis mechanism at low conversions.